OPTOELECTRONICS AND ADVANCED MATERIALS – RAPID COMMUNICATIONS Vol. 3, No. 4, April 2009, p. 297 - 304

Apodized chirped fiber Bragg gratings for wavelength shift compensation under sea level

O. MAHRAN*, T. A. HAMDALLAH, MOUSTAFA H. ALY[a], A. E. EL-SAMAHY
Faculty of Science, University of Alexandria, Alexandria, Egypt.
[a]*College of Engineering, Arab Academy for Science & Technology & Maritime Transport, Alexandria, Egypt, Member of the Optical Society of America (OSA)*

Bragg wavelength shift is numerically studied for different apodization profiles of chirped fiber Bragg grating (FBG). Linear and nonlinear cases are modeled and investigated. The values of the electric field and refractive index have been calculated using the numerical integration of the nonlinear coupled mode equation through Runge-Kutta method. Effects of temperature, pressure and strain under the sea level are studied together with the effect of nonlinearity. Finally, a zero shift has been obtained for each profile for enhancing the performance of FBGs.

(Received March 10, 2009; accepted April 23, 2009)

*Keywords:*Bragg grating fiber, Apodization, Dispersion compensation

1. Introduction

Fiber Bragg grating (FBG) is proving to be one of the most important recent developments in the field of the optical fiber technology. FBGs basically constitute generalized distributed reflectors whose reflection spectra and dispersion characteristics are wavelength-dependent and can be accurately adjusted by proper design. They can effectively be used for dispersion compensation in high-bit-rate, long-haul fiber communication links. The main peak in the reflection spectrum of a finite length Bragg gratings with uniform modulation of the index of refraction is accompanied by a series of side lobes at adjacent wavelengths. It is important in some applications to lower and if possible eliminate the reflectivity of these side lobes, or to apodize the reflection spectrum of the grating. For example, in the dense wavelength division multiplexing (DWDM), it is important to have a very high rejection of the nonresonant light in order to eliminate cross talk between information channels, and therefore, apodization becomes necessary.

The apodization of the fiber gratings using a phase shift mask with variable diffraction efficiency has been reported by Albert et al. [1]. A cosine apodization technique obtained by repetitive, symmetric longitudinal stretching of the fiber around the center of the grating, while the grating was written, has been recently reported by Kashyap et al. [2]. The simplicity of this technique allows the rapid production of fiber gratings required for the WDM systems and dispersion compensation [3].

2. Mathematical model

The refractive index variation is considered to be [4]:

$$n(z) = n_o\{1 + \sigma(z) + 2h(z)[\cos(2K_o z + \phi(z))]\}, \quad (1)$$

where n_o is the fiber refractive index, h(z) describes the amplitude variation of the induced refractive index modulation, σ(z) is the background refractive index variation, $K_o = 2\pi/\Lambda_o$ is the reference Bragg wave vector (Λ_o is the reference Bragg period), and φ(z) is the slowly varying grating phase. In the case of linearly chirped gratings, $\phi(z) = K_o C z^2$, where C (in m^{-1}) is the chirp parameter.

The total variation of the local Bragg wavelength across the entire grating length L is given by:

$$\Delta\lambda_B = 2\lambda_o CL, \quad (2)$$

where $\lambda_o = 2n_o\Lambda_o$ is the reference Bragg wavelength,

The amplitude variation, h(z), is, in general, expressed as:

$$h(z) = h_o f(x) \quad (3)$$

where h_o is the peak refractive index modulation and f(x) is the apodization profile.

The electric field distribution along the grating can be expressed in terms of two counter propagating waves as [5]:

$$E(z) = u(z)\exp\{-i[(\pi/\Lambda_o)z + (1/2)\phi(z)]\} + v(z)\exp\{+i[(\pi/\Lambda_o)z + (1/2)\phi(z)]\}, \quad (4)$$

where u(z) and v(z) are slowly varying amplitudes of the forward and backward traveling waves, respectively. The evolution of the amplitudes u(z) and v(z) is described by a set of two coupled differential equations, namely:

$$\frac{du(z)}{dz} = -[\delta(z)u(z) + k(z)v(z)], \tag{5-a}$$

and

$$\frac{dv(z)}{dz} = +[\delta(z)v(z) + k(z)u(z)], \tag{5-b}$$

with

$$\delta(z) = \Delta + \frac{\pi}{\Lambda_o}\sigma(z) - \frac{1}{2}\frac{d\phi}{dz}, \tag{6-a}$$

$$k(z) = \frac{\pi}{\Lambda_o}h(z), \tag{6-b}$$

and

$$\Delta = n_o k_o - \frac{\pi}{\Lambda_o}. \tag{6-c}$$

The parameters Δ and δ(z) represent the wave number detuning from the reference wave number π/Λ_o and the local detuning along the grating, respectively, and k(z) represents the local coupling constant. The boundary conditions of this particular scattering geometry are u(0) = 1 and v(L) = 0.

The main apodization profiles, considered in the present investigation are [6 and 7]:

1) Sine profile:

$$f(Z) = \sin^2(\frac{\pi z}{L}), 0 \le z \le L \tag{7}$$

2) Sinc profile:

$$f(x) = \frac{\sin(x)}{x}, \qquad x = \frac{2\pi(z - \frac{L}{2})}{L} \qquad 0 \le z \le L \tag{8}$$

3) Positive-Tanh profile:

$$f(x) = \tanh\left[\frac{2az}{L}\right], \qquad 0 \le z \le \frac{L}{2}$$

$$= \tanh\left[\frac{2a(L-z)}{L}\right], \qquad \frac{L}{2} \le z \le L \tag{9}$$

4) Blackman profile:

$$f(z) = \frac{1 + 1.19\cos(x) + 0.19\cos(2x)}{2.38}, \quad x = \frac{2\pi(z - \frac{L}{2})}{L}, \qquad 0 \le z \le L \tag{10}$$

5) Gauss profile:

$$f(x) = \exp\left[-G\left(\frac{z}{L}\right)^2\right], \qquad 0 \le z \le L \tag{11}$$

6) Hamming profile:

$$f(x) = \frac{1 + H\cos\left(\frac{2\pi z}{L}\right)}{1 + H}, \qquad 0 \le z \le L \tag{12}$$

7) Cauchy profile:

$$f(x) = \frac{1 - \left(\frac{2z}{L}\right)^2}{1 - \left(\frac{2Cz}{L}\right)^2}, \qquad 0 \le z \le L \tag{13}$$

2.1 Thermal effects

The center wavelength, λ_B, of the back-reflected light from a uniform FBG is defined by:

$$\lambda_B = 2\Lambda\, n_{eff}, \tag{14}$$

where Λ is the grating period and n_{eff} is the grating effective refractive index.

The shift, $\Delta\lambda_{BT}$, in the Bragg grating center wavelength due to temperature changes can easily be calculated using [8]:

$$\Delta\lambda_{BT} = 2\left(\Lambda\frac{\partial n_{eff}}{\partial T} + n_{eff}\frac{\partial\Lambda}{\partial T}\right)\Delta T, \tag{15}$$

where ΔT= (T-T_o), T(^oC) is the heating temperature and T_o(^oC) is a reference temperature.

Equation (15) can be rewritten in the form:

$$\Delta\lambda_{BT} = \lambda_o(\alpha_\Lambda + \alpha_n)\Delta T, \tag{16}$$

Where

$$\alpha_\Lambda = \frac{1}{\Lambda}\frac{\partial\Lambda}{\partial T},$$
$$\alpha_n = \frac{1}{n_{eff}}\frac{\partial n_{eff}}{\partial T}, \tag{18}$$

where λ_o is the fiber Bragg grating center wavelength at T_o, αΛ is the thermal expansion coefficient and α_n is the thermo-optical coefficient of the FBG.

The signal propagating with a high power causes a perturbation in the molecules resulting in a nonlinearity. So, in addition to the temperature effect, there is also the nonlinear effect on the selected wavelength. Therefore, the total change can easily be written as:

$$\Delta\lambda = \Delta\lambda_{nonlinaer} + \Delta\lambda_{BT}. \tag{19}$$

But, under the ocean depth, the temperature effect has a negative value. Therefore, the effect of the nonlinearity will appear as a compensator to the temperature effect as will be shown.

2.2 Strain effects

The shift, $\Delta\lambda_{BS}$, in the Bragg grating center wavelength due to strain changes can easily be calculated from [8]:

$$\Delta\lambda_{BS} = 2\left(\Lambda\frac{\partial n_{eff}}{\partial L} + n_{eff}\frac{\partial\Lambda}{\partial L}\right)\Delta L, \quad (20)$$

where ΔL is change in FBG length due to strain.

This shift, $\Delta\lambda_{BS}$, due to an applied strain on the FBG, can be expressed by:

$$\Delta\lambda_{BS} = \lambda_o(1-P_e).\Delta\varepsilon_Z, \quad (21)$$

with P_e the effective strain-optic constant defined as:

$$P_e = \frac{n_{eff}^2}{2}\{P_{12} - v(P_{11} - P_{12})\}, \quad (22)$$

where P_{11} and P_{12} are components of the strain-optic tensor, and v is Poisson's ratio. For a typical silica: fiber P_{11}= 0.113, P_{12}= 0.252, v= 0.16, and n_{eff} = 1.482 [8]. Using these values, the effective strain optic constant is found as P_e= 0.22.

Taking the nonlinear term into consideration, the total shift in the Bragg wavelength in the fiber Bragg grating can be written as:

$$\Delta\lambda = \Delta\lambda_{nonlinear} + \Delta\lambda_{BS}. \quad (23)$$

2.3 Strain and thermal effects

The Bragg grating resonance, which is the center wavelength of back reflected light from a Bragg grating, depends on the effective index of refraction of the core and the periodicity of the grating. The effective index of refraction, as well as the periodic spacing between the grating planes, will be affected by the changes in strain and temperature. The shift in the FBG center wavelength due to strain and temperature changes is given by:

$$\Delta\lambda_B = 2\left(\Lambda\frac{\partial n_{eff}}{\partial L} + n_{eff}\frac{\partial\Lambda}{\partial L}\right)\Delta L + 2\left(\Lambda\frac{\partial n_{eff}}{\partial T} + n_{eff}\frac{\partial\Lambda}{\partial T}\right)\Delta T. \quad (24)$$

The first term represents the strain effect on the optical fiber.

Including temperature, nonlinear and strain effects, one can write the total shift as:

$$\Delta\lambda = \Delta\lambda_{nonlinear} + (\Delta\lambda_{BT} + \Delta\lambda_{BS}). \quad (25)$$

The two terms between brackets will appear to cancel each other. In this case, the nonlinear term is the only effect on the Bragg wavelength.

2.4 Pressure effects

For a pressure change, ΔP, the shift, $\Delta\lambda_{BP}$, in the center wavelength is given by [8]:

$$\Delta\lambda_{BP} = \lambda_B\left[\frac{(1-2v)}{E} + \frac{n_{eff}^2}{2E}(1-2v)(2P_{12}+P_{11})\right]\Delta P, \quad (26)$$

where E is the Young's modulus of the elasticity of the fiber (=72 GPa). For normal silica fibers, the center FBG wavelength is 1550 nm and n_{eff}=1.482.

Similar to the above cases, when the nonlinear term appears together with the pressure influence, the total shift will be:

$$\Delta\lambda = \Delta\lambda_{nonlinear} + \Delta\lambda_{BP}. \quad (27)$$

2.5 The FBG under the seawater

Finally, when the fiber cable is found under the seawater, the pressure, temperature, and strain are changed in addition to the nonlinear effect and act to change the selected wavelength of the FBG. When all these parameters affect the Bragg wavelength, the total shift will be calculated from:

$$\Delta\lambda = \Delta\lambda_{nonlinear} + (\Delta\lambda_{BS} + \Delta\lambda_{BT} + \Delta\lambda_{BP}). \quad (28)$$

3. Results and discussion

3.1 Thermal effects

The effect of under sea level temperature on the different profiles of the apodized chirped Bragg grating appears in Figs. 1-7. The Figures show that all the nonlinear cases ($n_2 = 2.6\times10^{-20}$ m^2/W) have a shift more than that in the linear case. So, the nonlinearity acts as a compensator to the negative shift due to temperature.

In all profiles, in dashed lines, the positive shift and the negative shift are the same. Therefore, at an intermediate value for n_2, there will be a zero shift in the Bragg wavelength. From the table we can simplify the following:

	Linear Case $n_2 = 0$ m^2/W		Nonlinear Case $n_2 = 2.6\times10^{-20}$ m^2/W	
Apodization Profile	Room Temp.	Zero °C	Room Temp.	Zero °C
Blackman	0.19	-0.37	0.25	-0.27
Cauchy	0.09	-0.39	0.2	-0.29
Sinc	0.11	-0.31	0.21	-0.21
Sine	0.15	-0.35	0.25	-0.25
Tanh	0.18	-0.38	0.28	-0.28
Gauss	0.12	-0.34	0.22	-0.24
Hamming	0.04	-0.4	0.14	-0.31

Table 1. The shift in Bragg wavelength for different profiles under the effect of t he under seawater temperature.

1) In the linear case, at room temperature, Cauchy profile is the profile that will select the wavelength with a very small error, while Blackman profile is the profile of the maximum error in the wavelength selection.

2) In the nonlinear case, all profiles having a great error. The Hamming one is the profile that will select the wavelength with the lowest error. Also, the Tanh profile has the maximum shift in the wavelength selection.

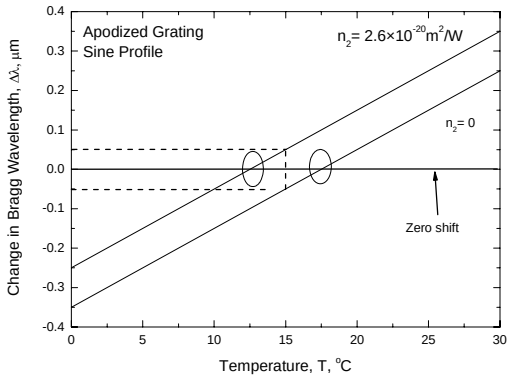

Fig. 1. Bragg wavelength shift as a function of temperature for Sine profile.

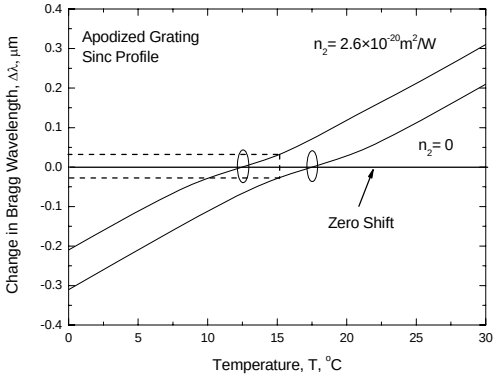

Fig. 2. Bragg wavelength shift as a function of temperature for Sinc profile.

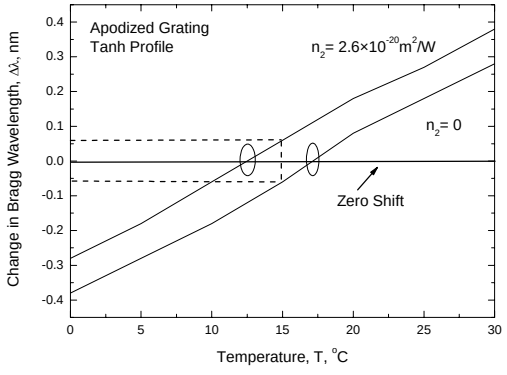

Fig. 3. Bragg wavelength shift as a function of temperature for Tanh profile.

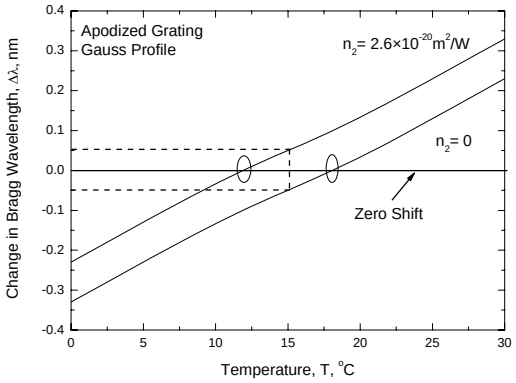

Fig. 4. Bragg wavelength shift as a function of temperature for Gauss profile.

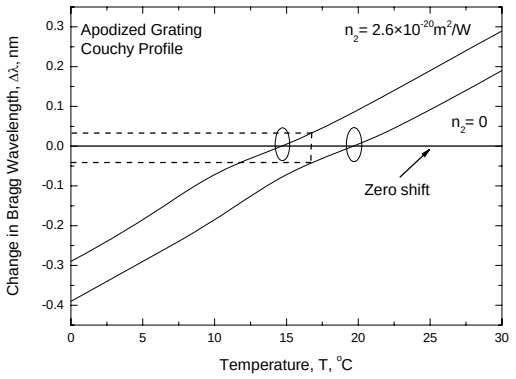

Fig. 5. Bragg wavelength shift as a function of temperature for Cauchy profile.

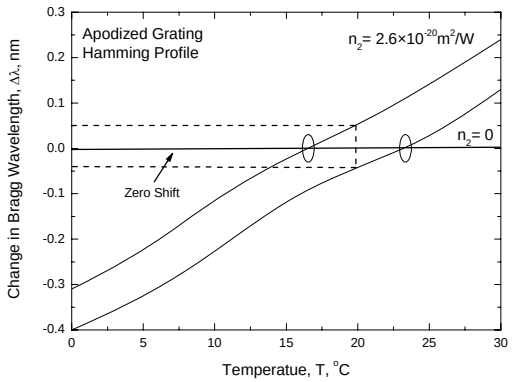

Fig. 6. Bragg wavelength shift as a function of temperature for Hamming profile.

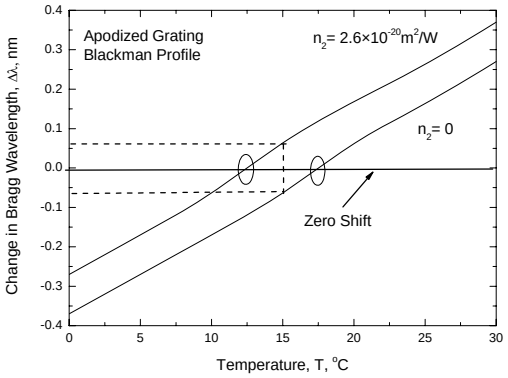

Fig. 7. Bragg wavelength shift as a function of temperature for Blackman profile.

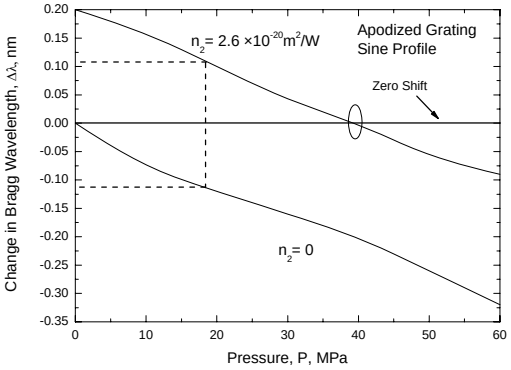

Fig. 9. Bragg wavelength shift as a function of pressure for Sine profile.

3.2 Pressure effects

The effects of the pressure change for the apodized chirped Bragg grating are displayed in Figs. 8-14. All profiles in the linear case appear with a negative shift that can be compensated by the strain except the small pressures in the Blackman and Tanh profiles. While in the nonlinear case (where n_2=2.6×10^{-20}m^2/W), all the profiles below 20 MPa have a positive shift with no compensation and after 20 MPa, some of the profiles begin to take a negative values and must be compensated. Comparing all profiles, so we can note the following:

1) In the linear case, the sine profile is the recommended profile to select the wavelength with no shift (at the sea level), while the tanh profile has the maximum shift with a very poor wavelength selection.

2) In the nonlinear case, all profiles are very poor in the wavelength selection. The Gaussian profile is considered to have the smallest error.

3)

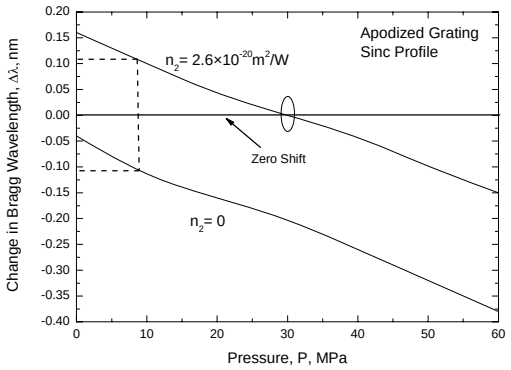

Fig. 10. Bragg wavelength shift as a function of pressure for Sinc profile.

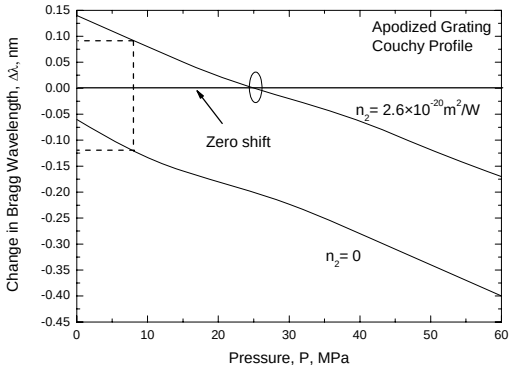

Fig. 8. Bragg wavelength shift as a function of pressure for Cauchy profile.

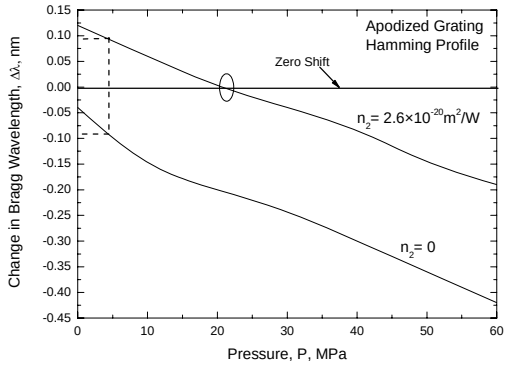

Fig. 11. Bragg wavelength shift as a function of pressure for Hamming profile.

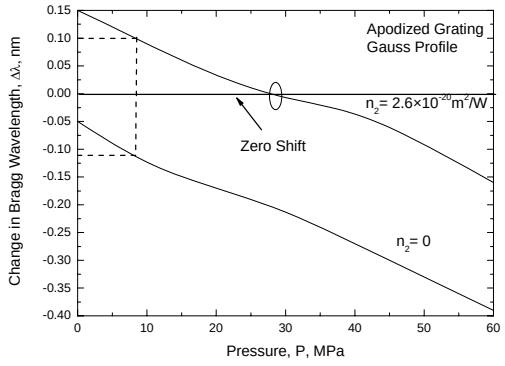

Fig. 12. Bragg wavelength shift as a function of pressure for Gauss profile.

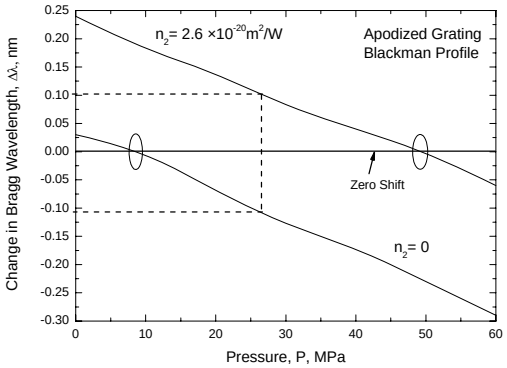

Fig. 13. Bragg wavelength shift as a function of pressure for Blackman profile.

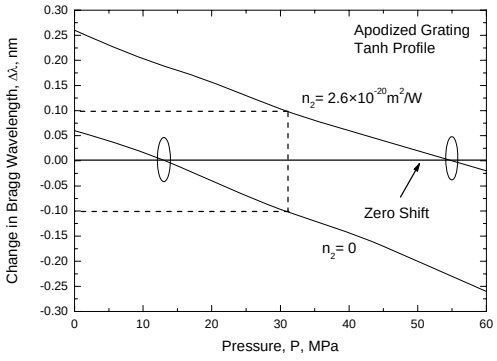

Fig. 14. Bragg wavelength shift as a function of pressure for Tanh profile.

3.3 Ocean depth effect

Under the ocean depth, both temperature and pressure change with certain values. The chosen values of the ocean depth and its pressure and temperature change are obtained from [9]. Fig. 15 shows the change in Bragg wavelength as a function of the ocean depth in the linear case where ($n_2 = 0$). The solid line shows the optimum values of the zero shifts in the Bragg wavelength which is the optimum value for the Bragg grating to select any wavelength without any error for the low power signal (the linear case). Figure 16 shows the nonlinear behavior where a high power signal transmits through the Bragg grating. Obviously, the zero shift is between 1500 and 4000 m under the sea level.

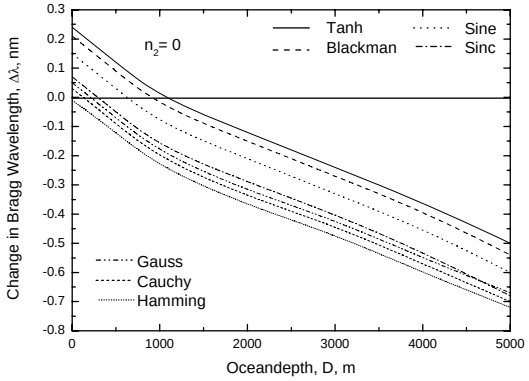

Fig. 15. Bragg wavelength shift as a function of ocean depth for linear case.

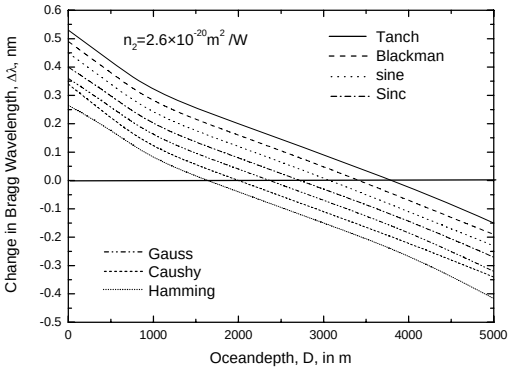

Fig. 16. Bragg wavelength shift as a function of ocean depth for nonlinear case.

3.4 Wavelength shift compensation by using the strain effects

Figs. 17 and 18 display the applied strain with temperature that compensates the temperature effect reaching to a Bragg wavelength compensation, $\Delta\lambda = 0$, for the linear and nonlinear cases, respectively.

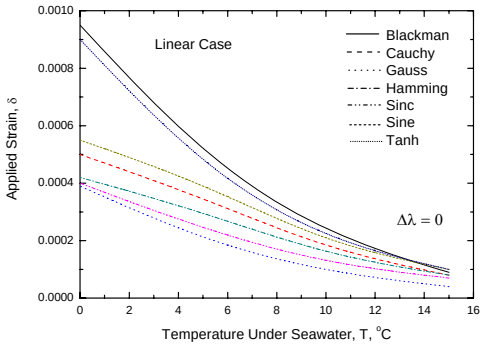

Fig. 17. The change of the applied strain with the temperature under the sea level to obtain a zero shift.

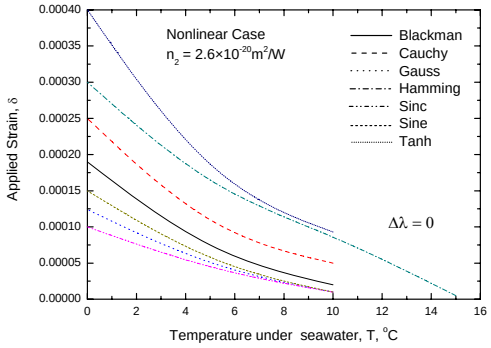

Fig. 18. The change of the applied strain with the temperature under the sea level to obtain a zero shift.

Similarly, Figs. 19 and 20 display the applied strain with pressure that compensates the pressure effect reaching to a Bragg wavelength compensation, $\Delta\lambda = 0$, for the linear and nonlinear cases, respectively. In Fig. 19, the calculations done for the written profiles only while the other profiles have a positive shift. So, they cannot be compensated using the strain effect. Therefore, in these profiles, the nonlinearity will be the only compensator.

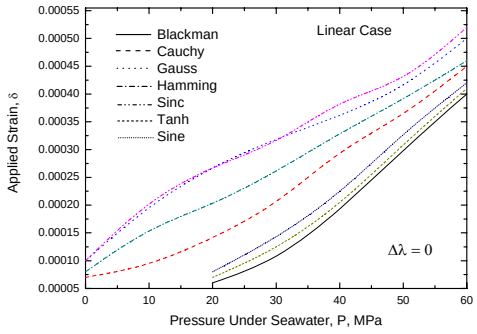

Fig. 19. The change of the applied strain with the pressure under the sea level to obtain a zero shift.

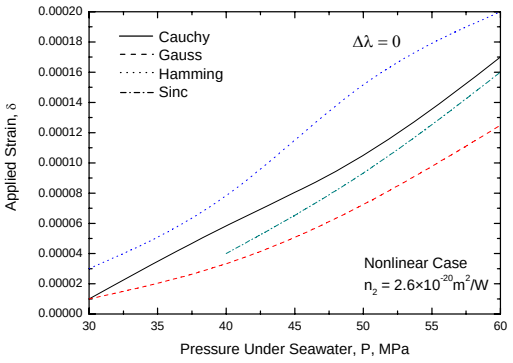

Fig. 20. The change of the applied strain with the pressure under the sea level to obtain a zero shift.

Finally, Figs. 21, 22 display the compensation $\Delta\lambda = 0$ due the existence of the Bragg grating under the sea level where there is double shift coming from the change in pressure and temperature in the linear case. While

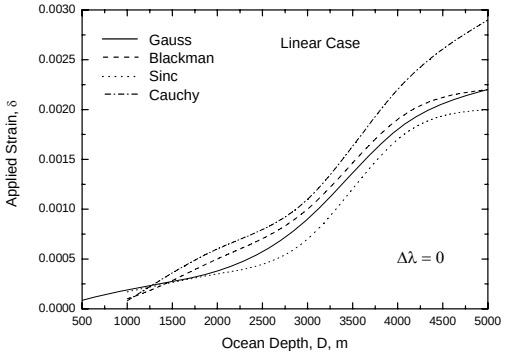

Fig. 21. The change of the applied strain with the ocean depth.

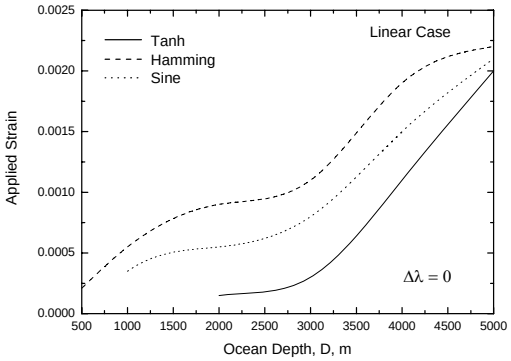

Fig. 22. The change of the applied strain with the ocean depth.

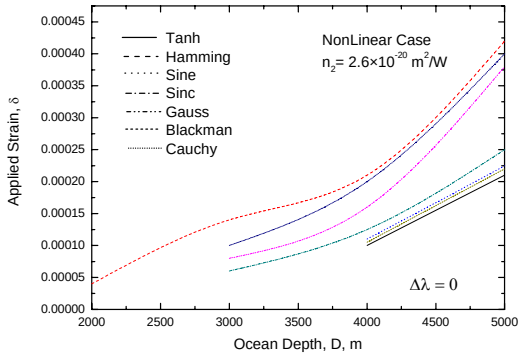

Fig. 23. The change of the applied strain with the ocean depth.

Fig. 23 shows the compensation in the high power signals (nonlinear case).

4. Conclusions

The compensation of the Bragg wavelength shift for the apodized chirped Bragg grating is studied and investigated. It is shown that the applied strain can be used as a compensator to the shift in Bragg wavelength for all types in apodized grating in the linear case. In the nonlinear case, the nonlinearity can act as a compensator to the wavelength shift.

References

[1] J. Albert, K. O. Hill, B. Mallo. Electron. Letters **31**, 222 (1995).
[2] Kashyap, R. A. Swanton, D. J. Armes, Electron. Letters **32**, 1226 (1996).
[3] J. Albert, R. Kain, Electron. Letters **32**, 2260 (1996).
[4] K. O. Hill, G. Meltz, J. Lightwave Technol. **15**, 1263 (1997).
[5] A. Othonos, K. Kalli, Fiber Bragg Gratings, 2nd ed., Artech House, Norwood, 1999.
[6] E. Karin, J. Mikhail, R. Laming, J. Quantum Electronics **34**, 770 (1998).
[7] D. Pastor, D. Ortega, V. Tatay, J. Lightwave Technol. **14**, 2581 (1996).
[8] K. O. Hill, G. Meltz, J. Lightwave Technol. **15**, 1263 (1997).
[9] G. Ghosh, H. Yajima, J. Lightwave Technol. **16**, 2002 (1998).

* Corresponding author: O_Mahran2003@yahoo.com